SUPPLEMENTAL INFORMATION

Supplemental information includes seven figures and five tables that can be found with the article online at ***

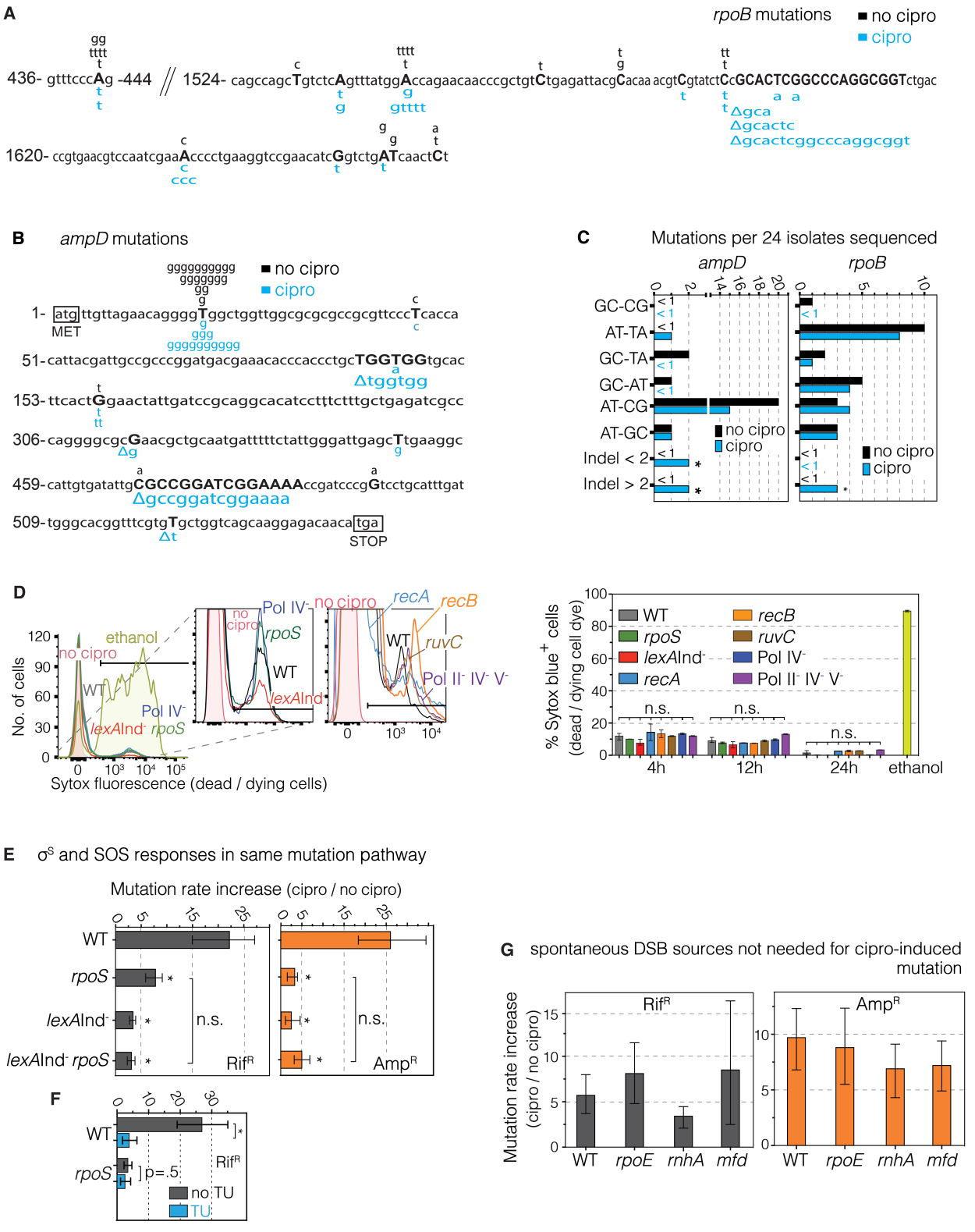

Figure S1. Mutation Sequences, a Single Pathway (Epistasis), and Independence from Spontaneous DSB Generators, Related to Figures 1, 2

(A) RifR cfu carry *rpoB* base-substitution mutations found in two clusters. These cause amino-acid changes that reduce rifampicin binding to the RpoB RNA polymerase subunit. Black, spontaneous; blue cipro-induced mutations.
(B) AmpR cfu carry *ampD* loss-of-function mutations. Summary of mutation sequences from independent AmpR clones, isolated from cipro-induced and spontaneous mutants. *ampD* loss-of-function mutations confer AmpR to *E. coli* strain carrying a chromosomal cassette of Enterobacter *ampRC* genes (Petrosino et al., 2002) (**Methods**) by allowing constitutive expression of the AmpC beta-lactamase, which confers resistance. Black, spontaneous, blue; cipro-induced mutations.
(C) Indels are more abundant in cipro-promoted than spontaneous mutations, **p*<0.001, Chi-squared test. Sequences from 24 independent isolates grown in the absence or presence of cipro MAC. There were significantly fewer 8-oxo-dG-signature mutations (G·C→T·A and A·T→C·G) in cells grown with cipro compared with no cipro, *p=0.01, two-tailed Student's *t*-test. Counts of 24 independent RifR and AmpR isolates; * <1 indicates zero mutations of the type indicated among the 24 isolates, i.e., < 1 per 24 is < 4%.
(D) SYTOX blue detection of dead/dying cells shows that cell death frequencies at MAC cipro concentrations per mutagenesis experiments (Table S1, all strains) are similar for the strains used, obviating potential concerns about death inflating apparent mutation rates (Frenoy and Bonhoeffer, 2018). Thus the concern of Frenoy and Bonhoeffer (2018) that bacterial cell death might cause overestimation of apparent antibiotic-induced mutation rates, predicted by their mathematical modeling, cannot account for the higher mutation rate in WT than MBR-mutant strains (Figure 1F). Additionally, it cannot account for the difference between the large σ^S low-activity (non-mutagenic) cell subpopulation and the small σ^S high-activity (mutagenic gambler) cell subpopulation, which show similar death levels (Figure S7C). We note also that the mathematical modeling of (Frenoy and Bonhoeffer, 2018) showed no such potential inflation of mutation rate in the case of either—(i) a cell subpopulation producing most mutants; or (ii) multi-chromosome cells (Frenoy and Bonhoeffer, 2018), both of which are true for cipro-induced cross-resistance mutagenesis (Figure 4A-C and Figure 7B, respectively).
(E) The SOS and general σ^S stress responses are epistatic for mutagenesis, i.e. act in the same mutation pathway. MAC doses, Table S1; raw mutation rates, Table S2. Means ± 95% confidence intervals of n≥ 3 independent experiments. *Differs from WT value, *p*<0.01, one-way ANOVA with Tukey's post-hoc test of natural-log transformed data.
(F) Thiourea (TU) does not reduce mutagenesis further in Δ*rpoS* cells, which lack σ^S, implying that ROS promote mutagenesis in the σ^S-response-dependent mutation pathway. MAC doses, Table S1; raw mutation rates, Table S2. Data and statistics per (E).
(G) Proteins that promote spontaneous DSBs required for starvation stress-induced MBR are not required for cipro-induced MBR. The σ^E (RpoE) membrane stress response (Gibson et al., 2010) and RNA-DNA hybrids (Wimberly et al., 2013) in starvation-stress-induced MBR. RNA-DNA-hybrid removal by RNase HI (*rnhA*), and prevention by loss of Mfd (which dislodges stalled RNA polymerases) promote DSBs and underlie about half of starvation stress-induced MBR (Wimberly et al., 2013), but neither is required for MBR instigated by cipro, supporting the hypothesis that cipro-provoked DSBs drive mutagenesis. Mutation rates estimated using the MSS-maximum likelihood method. Data and statistics per (E). MAC doses, Table S1; raw mutation rates, Table S2.

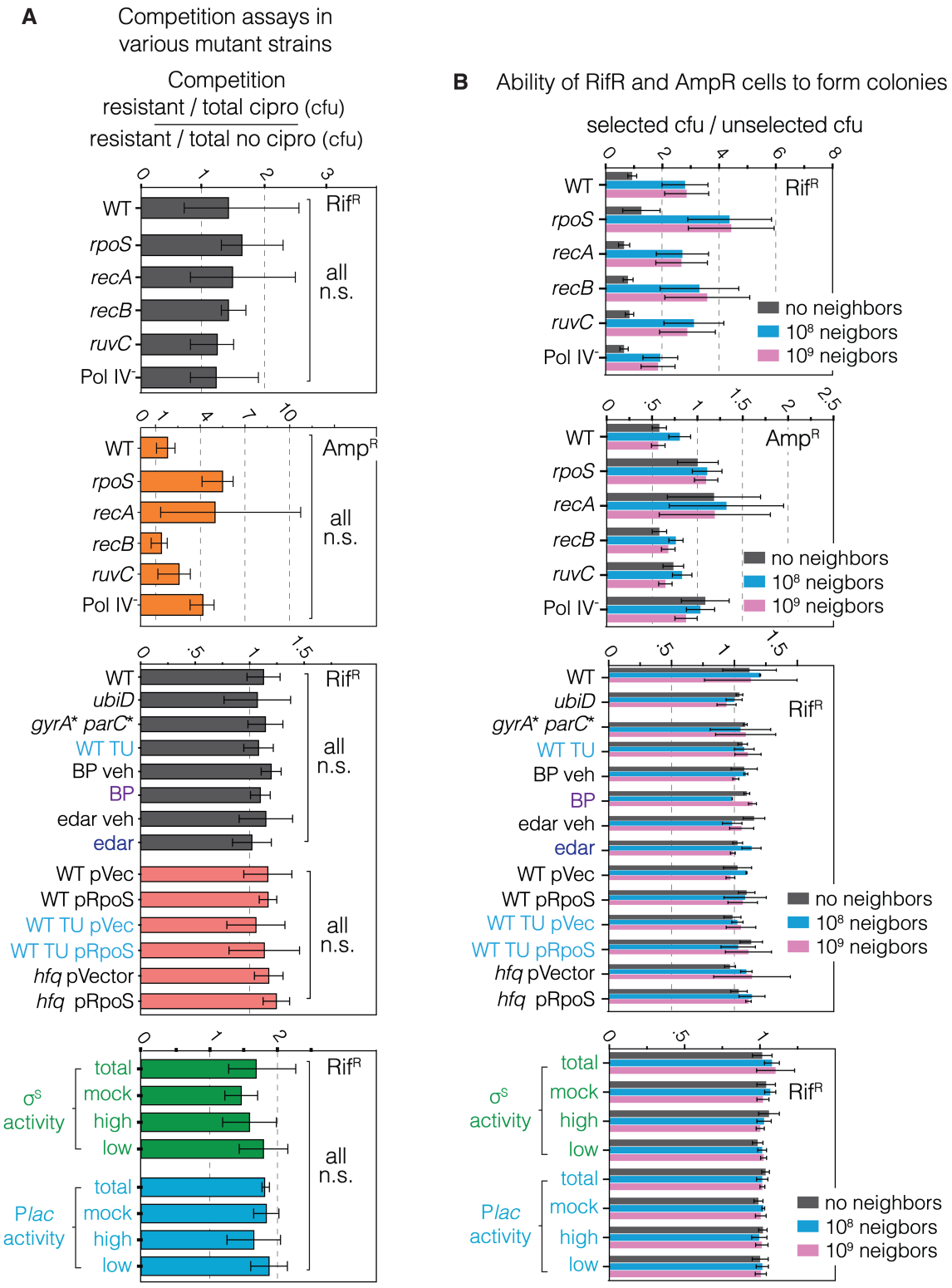

Figure S2. No Growth or Colony-Formation Defects in Rifampicin- and Ampicillin-Resistant Mutants, Related to Figures 1, 2, 3, 4, 5, 6, 7

We excluded the possibility that possible reduced growth rates of MBR-defective-mutant strains, or ROS-scavenged cells, in cipro, or as colonies on Rif and Amp plates after cipro might cause

artificial apparent reductions in mutant frequencies (used to estimate mutation rates) for various mutants tested. We show no growth disadvantage in cipro of RifR or AmpR MBR-mutant or ROS-scavenged cells relative to wild-type (WT) unscavenged cells, and no defect in forming colonies afterward. Cells grown with or without MAC cipro; Table S1 for MACs all strains.
(A) RifR or AmpR derivatives of mutant strains assayed are not more disadvantaged by cipro than WT cells, indicating that RifR or AmpR mutant cfu in these strains reflects reduced mutagenesis, not inability of the RifR or AmpR mutants to survive the assay relative to WT cells. Competition assays measuring percent of RifR or AmpR cells in culture after growth to saturation under conditions identical to mutation assays in the absence or presence of cipro MAC. Initial conditions were 50% sensitive and 50% resistant cells. A value of 1 indicates no difference in growth. Mean and 95% CI of ≥ 3 independent experiments. For σ^S- and *lac*-activity bar graphs, data are mean ± range of 2 independent experiments. n.s., not significantly different from the wild-type value at $p<0.01$ one-way ANOVA with Tukey's post-hoc test.
(B) Reconstruction experiments show that RifR and AmpR derivatives of the MBR- and other-mutant strains assayed form colonies as well as those in the WT background, under reconstructions of selective conditions. Thus, reductions in RifR or AmpR mutant cfu in strains assayed reflect reduced mutagenesis relative to the WT background, not inability of the RifR or AmpR derivatives to form colonies when selected. Cells from RifR or AmpR colonies were plated on LBH medium with rifampicin or ampicillin respectively with varying amounts of antibiotic-sensitive neighbor cells, and on LBH plates without antibiotics to determine cfu. During selection for RifR or AmpR cfu in mutagenesis experiments, sensitive neighbor cells are present on initial contact with the drug selection plates, and are expected to die over time from exposure to rifampicin or ampicillin. A value of 1 indicates no deviation in the number of cfu scored in the presence of rifampicin or ampicillin from those without the drugs. If greater than 1, more resistant cfu appeared under selective conditions than on no-drug plates. If less than 1, fewer mutant cells were able to form cfu on drug plates than no-drug plates. None of mutants tested showed inhibition of colony formation relative to the WT, indicating that reductions of cfu reflect reduced mutagenesis, not reduced mutant-cell outgrowth. Mean ± 95% CI of at least 3 independent experiments. For σ^S activity and *lac* activity bar graphs, data represent mean ± range of 2 independent experiments, none was significantly different from WT, one-way ANOVA with Tukey's post-hoc test.

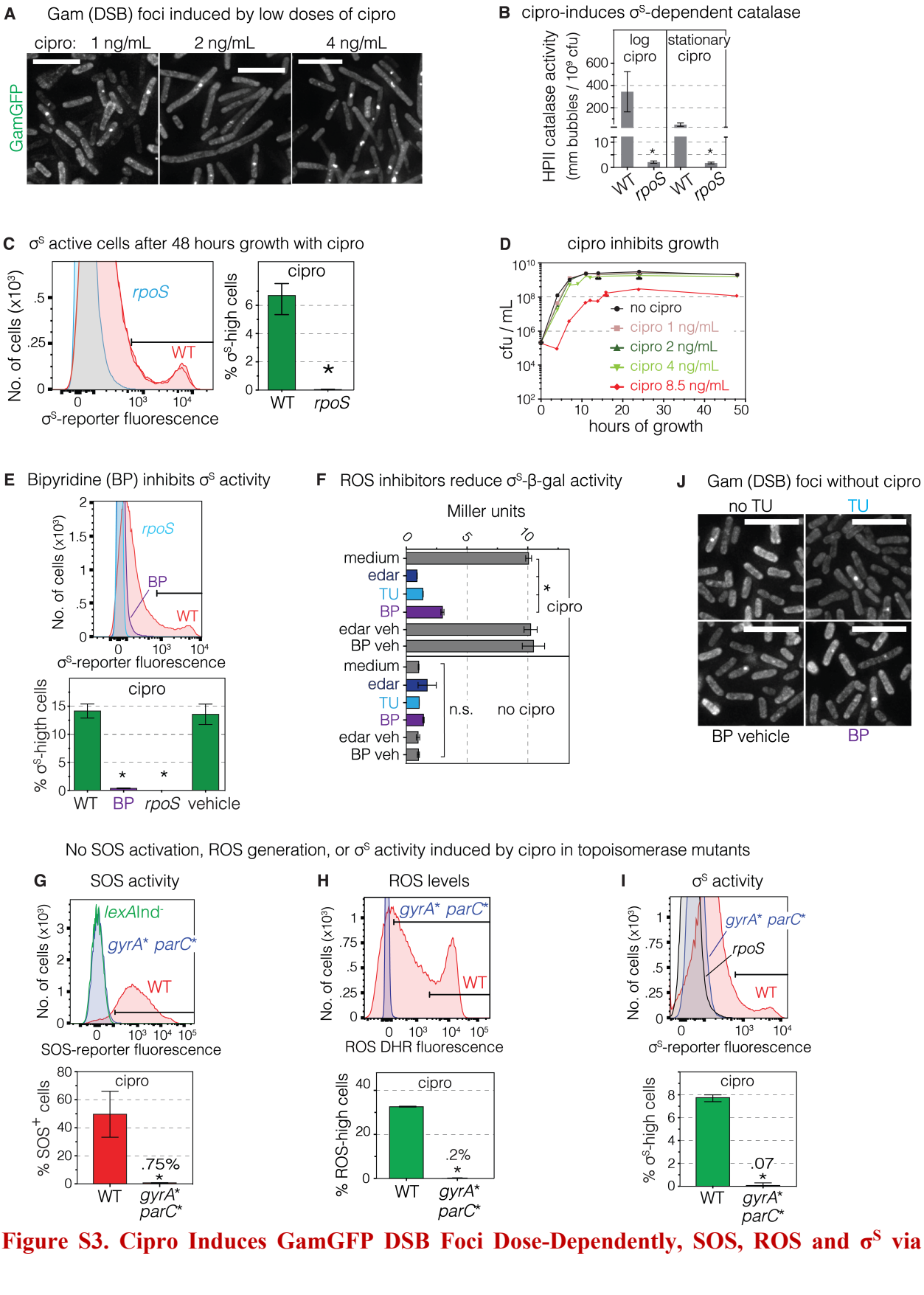

Figure S3. Cipro Induces GamGFP DSB Foci Dose-Dependently, SOS, ROS and σS via

Binding Target Topoisomerases, and Inhibition of σ^S Activity by ROS Reducers, Related to Figures 1, 2, 3

(A) Cipro induces GamGFP DSB foci dose dependently. Representative images of GamGFP foci in log-phase cells quantified, Figure 1G. Scale bar, 5µm.

(B) The σ^S-dependent HPII catalase activity is induced by MAC cipro in both log- and stationary-phase cells. HPII measured as bubbles per 10^9 cells. Means ± SEM, 3 experiments. *Differs from WT, $p<0.01$, one-way ANOVA with Tukey's post-hoc test.

(C) σ^S high gambler subpopulation persists to 48h growth in MAC cipro (AmpR assays conditions). *yiaG-yfp* reporter. Means ± range, 2 experiments. *Differs from wild-type (WT), $p<0.01$, two-tailed Student's *t*-test.

(D) Dose response of growth inhibition by cipro. Where not visible, error bars are smaller than the symbol. Means ± range, ≥2 experiments.

(E) ROS are required for cipro induction of σ^S-response activity. ROS-preventing agent 2,2' bipyridyl (BP, 0.25mM) inhibits MAC cipro induction of σ^S activity, flow cytometric assay of stationary phase cells (24h) carrying the *yiaG-yfp* σ^S-response reporter. Afu, arbitrary fluorescence units. Means ± range, 2 experiments. *Differs from WT, $p<0.01$, one-way ANOVA with Tukey's post-hoc test.

(F) ROS are required for cipro-induced accumulation of σ^S, assayed as σ^S-beta-galactosidase activity in stationary-phase cells (24h). *Differs from WT, $p<0.01$, one-way ANOVA with Tukey's post-hoc test.

(G-I) Cipro binding to its target type-II topoisomerases is required for activation of (G) the SOS response, (H) generation of ROS, and (I) activation of the σ^S response. The *gyrA** and *parC** mutant alleles encode subunits of gyrase and Topo IV, respectively, that are functional but are not bound by cipro. Representative flow cytometry histograms, SOS (stationary phase 24h), σ^S activity (stationary phase 24h), and ROS (log phase 16h) in strains carrying the chromosomal SOS reporter P_{sulA}*mCherry*, σ^S-response reporter *yiaG-yfp*, or stained with the DHR ROS dye. Means ± range, 2 experiments. *Differs from WT, $p<0.01$, two-tailed Student's *t*-test.

(J) Spontaneous GamGFP foci form independently of ROS (control for cipro-treated cells, Figure 2H). Ferrous iron chelator 2,2' bipyridyl (BP) inhibits ROS-forming Fenton reactions. Thiourea (TU) scavenges hydroxyl radicals. Cells imaged in log-phase. Scale bar, 5µm.

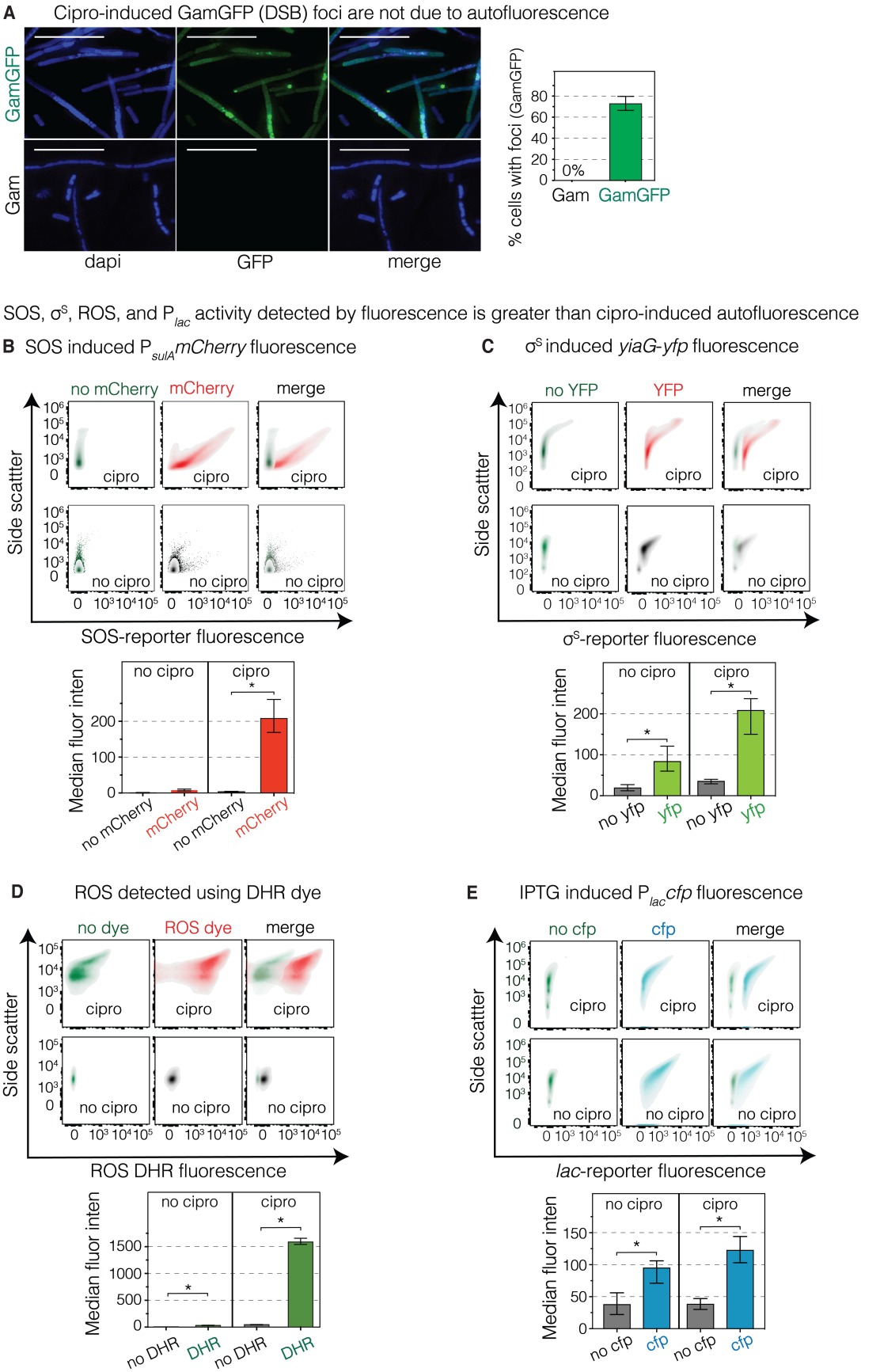

Figure S4. Fluorescence Data Exceed Cipro-Induced Autofluorescence, Related to Figures 1,

2, 3, 4, 5, 6

(A) Autofluorescence induced by cipro does not cause foci. Control for Figures 1G, 2H, and 3F. Cells that produce Gam or GamGFP were grown in MAC 8.5ng/mL cipro and imaged in log phase, 16h. Only cells with GamGFP turn green and form foci. ≥ 200 cells quantified per experiment.

(B-E) Autofluorescence is not responsible for cipro-promoted fluorescence-reporter activities in flow-cytometric assays. Autofluorescence has been reported in bacterial cells treated with bactericidal antibiotics (Renggli et al., 2013). We compared MAC cipro-treated cells without and with the reporters of—

(B) the SOS response (Δ*attλ*::P_{sulA}*mCherry*);

(C) σ^S activity (*yiaG-yfp*);

(D) ROS, DHR ROS dye; or

(E) control, P_{lac}*cfp* activity induced by IPTG (1mM). Cipro-induced autofluorescence in cells without fluorescence reporters in the red, yellow, green, and cyan emission wavelengths produce less fluorescence than the positive-fluorescence readings in cells with the chromosomal fluorescence reporters, or ROS staining. The autofluorescence does not overlap with induced fluorescence signals. MAC cipro-grown cells assayed in stationary phase, 24h.

A-E, Mean ± range, 2 experiments. *Different from WT, $p<0.01$, (A) two-tailed Student's *t*-test, and (B-E) one-way ANOVA with Tukey's post-hoc test.

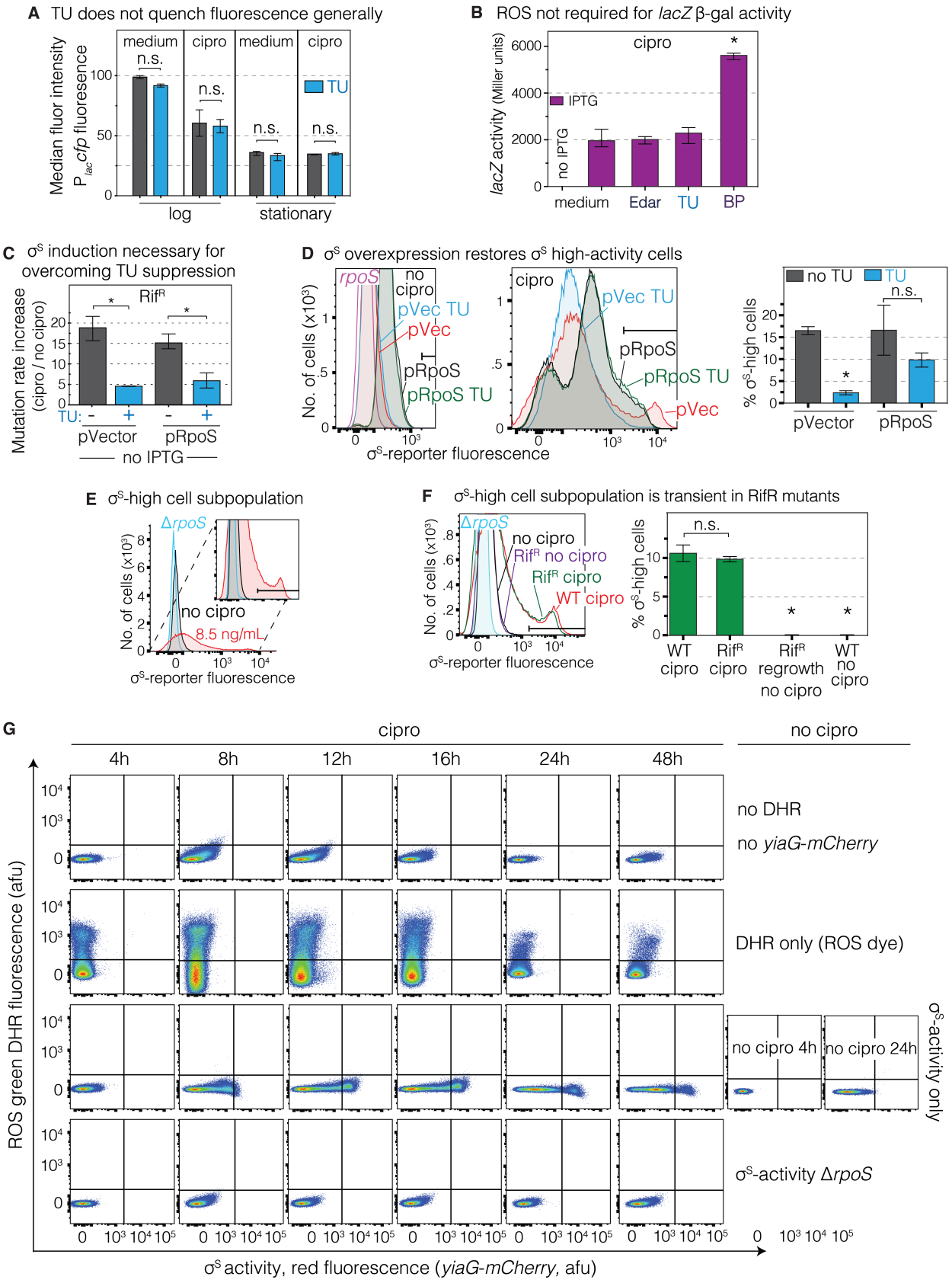

Figure S5. No Effect of ROS Reducers on β-gal Activity or Fluorescent-Protein Activation;

IPTG Induction of σ^S Substitutes for ROS in Mutagenesis; and Single and No Fluorescence Controls for ROS and σ^S Detection in Same Cells, Related to Figures 2, 3, 4, 5

(A) Thiourea (TU) does not inhibit accumulation of IPTG-induced fluorescence from P_{lac}*cfp* reporter, under conditions of the mutation assays in log or stationary phase. Negative control for Figures 2E and 4A. Means ± range, 2 experiments. n.s. not significant, one-way ANOVA with Tukey's post-hoc test.

(B) ROS are not required for *lac*-reporter activity. ROS reducers TU, BP, and edaravone do not inhibit β-galactosidase induction or activity. Cells grown with IPTG (100mM), in MAC cipro and TU, BP, or edaravone for 24h. Negative control for Figure 5E. Means ± range, 2 experiments. *Differs from no-cipro control IPTG value, $p<0.01$, one-way ANOVA with Tukey's post-hoc test.

(C) Induction of *rpoS* transcription is required for σ^S substitution for ROS in mutagenesis. TU inhibition of mutagenesis (100 mM) is not suppressed in cells with pRpoS plasmid if no IPTG is added. Negative control for Figure 2G. Means ± range, 2 independent experiments. *Differs as indicated, $p<0.01$, one-way ANOVA with Tukey's post-hoc test.

(D) Production of σ^S from a plasmid restores σ^S activity to appropriate levels, not abnormally high, in TU-treated cells. The plasmid-produced σ^S activity is not as high as in cultures without TU, though it has a comparable fraction of cells higher than the gate of FACSed σ^S-high cells that produce mutants (Figure 3A). The plasmid-produced σ^S is also unaffected by ROS/TU, as expected. The absence of the very highest intensity σ^S-high cells with the plasmid suggests that σ^S production reduces ROS, and so the very highest σ^S levels induced by ROS, through its upregulation of antioxidant activities. Negative control for Figures 2G, 5D, 6B, show that restoration of mutagenesis to TU-quenched, Hfq- or UbiD-defective cells by σ^S production does not reflect abnormally high-levels of σ^S from the plasmid used. Cells grown in MAC cipro, assayed at 24h. Means ± range, 2 independent experiments. *Differs from pVector no TU, $p<0.05$, two-tailed Student's *t*-test.

(E) Cipro-induced cells have higher σ^S activity than stationary phase cells grown without cipro. Representative flow cytometry histogram of σ^S activity from *yiaG-yfp* in Δ*rpoS* and in WT cells grown with and without MAC cipro, assayed at 24 hours. No-cipro cells have higher σ^S-activity than Δ*rpoS* cells, and MAC cipro-treated cells have much higher activity than no-cipro cells.

(F) The σ^S-high state of gamblers is transient, shown with the σ^S-response reporter *yiaG-yfp*. Four independent cipro-induced RifR mutants isolated and grown for 24h show no greater σ^S activity than their RifS parent, which did not arise specifically in a gambler population. Means ± range, 2 experiments. *Differs from WT, $p<0.01$, one-way ANOVA with Tukey's post-hoc test.

(G) No fluorescence and single-color negative controls experiments in Figure 4A and B. Cells harvested for flow cytometry serially from cultures at 4, 8, 12, 16, and 24 hours after addition of MAC cipro. Representative flow-cytometry plots from 3 experiments.

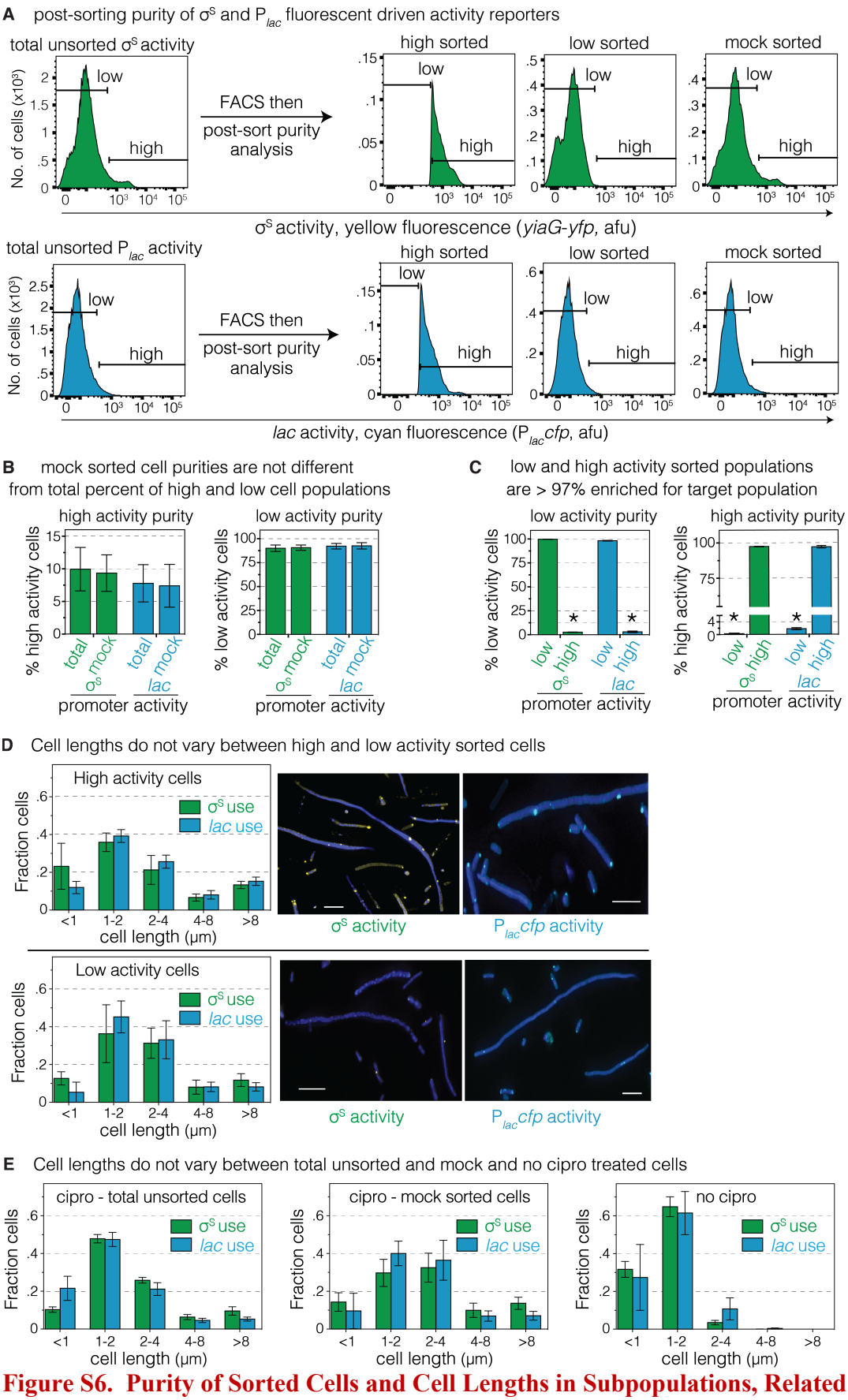

Figure S6. Purity of Sorted Cells and Cell Lengths in Subpopulations, Related to Figure 3

(A) Sorted cell populations are at least 97% pure. Post-sort purity checks verify expected fluorescence intensities in cells in mock-sorted, and low- and high-fluorescence sorted cell populations. Cells grown for 24h in MAC cipro before sorting.
(B and C) Quantification of post-sort purity. Mean ± range, 2 experiments; * $p<0.0001$, one-way ANOVA with Tukey's post-hoc test.
(D and E) Cell lengths do not differ between *lac*-reporter and *yiaG-yfp* σ^S-reporter sorted populations. Mean ± SD, 3 experiments of > 300 cells each. Not different, one-way ANOVA with Tukey's post-hoc test.
(D) σ^S- or -β-galactosidase-high and low activity sorted cells. Representative merged images of DAPI DNA staining and either CFP (β-gal) or YFP (σ^S) fluorescence and quantification of cell lengths. Scale bar, 5μM.
(E) Unsorted, mock-sorted, and untreated cell controls.

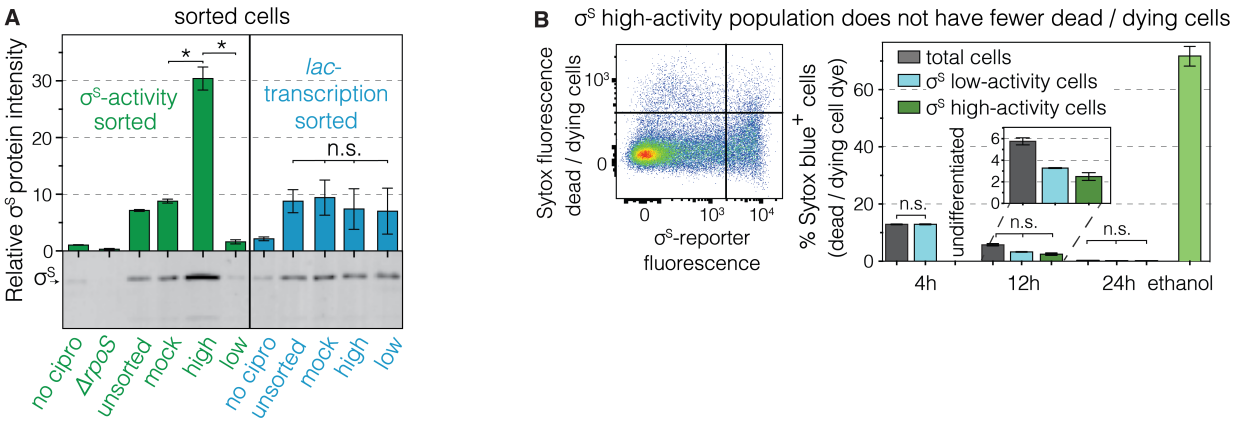

C Cipro-induced Rif^R mutants are not heritably mutator

Strain	# independent cultures (1 spot per culture)	Nal^R colonies per spot	Strain	# independent cultures (1 spot per culture)	Nal^R colonies per spot
WT parent	2	0.5 ± 1[b]	Rif^R mutant-5	2	< 0.5[b]
WT parent[a]	8	0.7 ± 1[b]	Rif^R mutant-6	2	< 0.5[b]
mutS	2	42 ± 4	Rif^R mutant-7	2	0.5 ± 1[b]
Rif^R mutant-1	2	< 0.5[b]	Rif^R mutant-8	2	< 0.5[b]
Rif^R mutant-2	2	0.5 ± 1[b]	Rif^R mutant-9	2	< 0.5[b]
Rif^R mutant-3	2	0.5 ± 1[b]	Rif^R mutant-10	2	< 0.5[b]
Rif^R mutant-4	2	< 0.5[b]			

[a]This is parent exposed to cipro as in a cipro-induced mutagenesis experiment, then isolated after the experiment on no-drug plates. This parallels the Rif^R mutants, which came from cipro-induced mutagenesis experiments.

[b]Differs from *mutS* mutator strain, p<0.0001, one-way ANOVA with Tukey's post-hoc test.

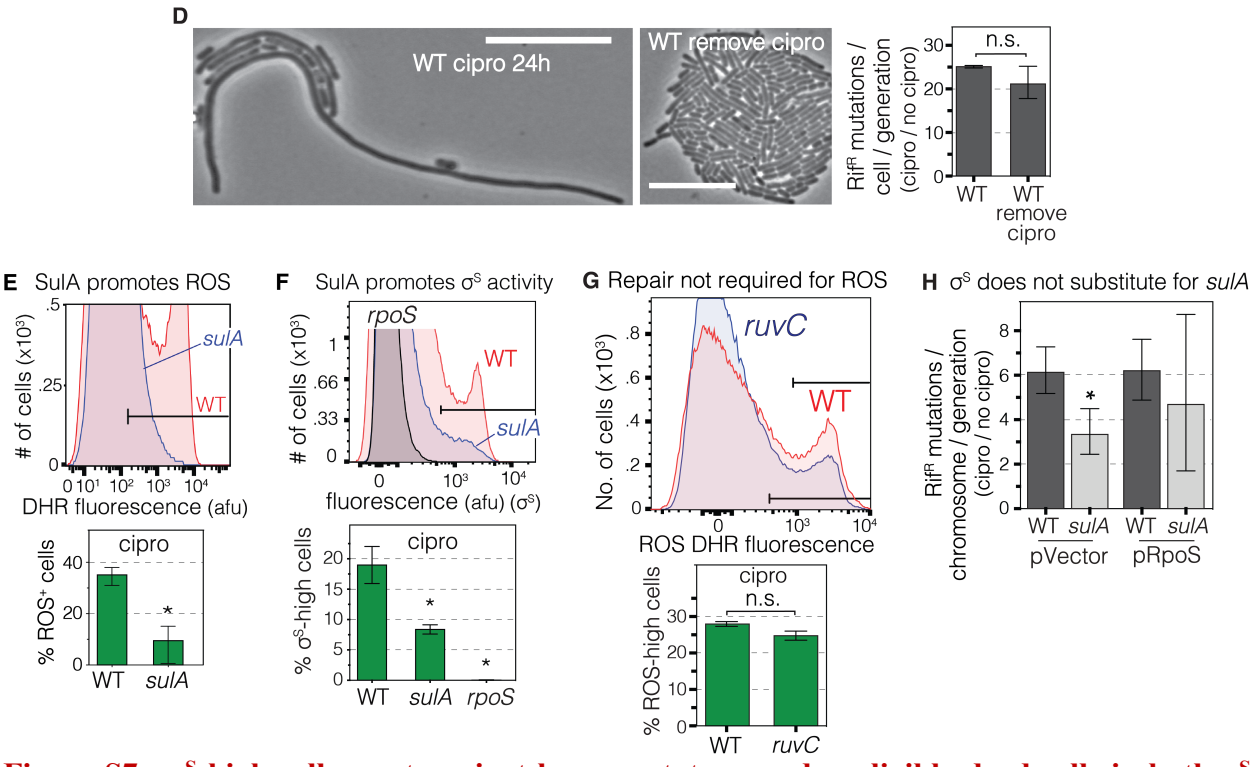

Figure S7. σ^S-high cells are transient hypermutators, and negligible dead cells in both σ^S

high- and low-activity cell populations, Related to Figures 2, 3, 6, 7

(A) High σ^S protein levels in FACS sorted σ^S-high-activity cells. Western blots from cell subpopulations at 24h in MAC cipro. Means ± SEM, 3 experiments. *p<0.01, one-way ANOVA with Tukey's post-hoc test; n.s., not significant. Additionally, we verified that FACS sorted fluorescent σ^S-reporter carrying cells had high σ^S activity by showing that they displayed significantly higher levels of σ^S-dependent catalase activity (Figure 3B) than the cells in the low-fluorescence or mock-sorted populations, and also had more σ^S protein accumulation (Figure S7A). Microscopic analyses showed that the σ^S-response-high and -low cells did not differ detectably in cell lengths or sizes (Figure S6D,E).

(B) Cell death is not different in σ^S high- or low-activity cell subpopulations in MAC cipro. Flow cytometry assay for cell death in log phase (4h and 12h) and stationary phase (24h) of strains with the *yiaG-mCherry* σ^S-response reporter stained with SYTOX blue dead-cell stain, quantifies single cells with dye-permeable membranes. Representative flow cytometry distribution. Means ± range, 2 experiments. n.s., not significant, one-way ANOVA with Tukey's post-hoc test.

(C) Cipro-induced RifR mutants are not heritably mutator. Nalidixic-acid-resistance-mutagenesis assay. Two independent cultures of the wild-type parent, stable mutator (mismatch repair defective *mutS*), and 10 different cipro-induced RifR mutant isolates were spread on plates, then spotted with nalidixic acid, incubated, and NalR mutant papillae in the zones of inhibition counted. *Differs from *mutS* mutator strain, p<0.0001, one-way ANOVA with Tukey's post-hoc test. The data show that the state of increased mutagenesis in σ^S-active gambler cells (Figure 3A) is transient, and not a heritable mutator state.

(D) Cipro induces mutagenesis in transient cipro treatment experiments. Cells were grown as for cipro-induced mutagenesis experiments in MAC cipro except that at 18-19 hours, cells were removed from the cipro and grown without cipro (37° shaking as for mutagenesis experiments) for 4-6h to allow resolution of multi-chromosome cell filaments into individual small cells, then plated for total and RifR cfu and mutation rates estimated. The data show that cipro induction of mutation rate is not a consequence of cfu in the cipro-treated cultures containing more chromosomes than in untreated cells, which do not filament. These data support the conclusion that mutation rate *per chromosome* is increased by cipro, as shown independently, (**Figure** 7G, and Table S4). Representative brightfield microscopy images show the resolution of filaments in WT removed from cipro at 18 hours and grown in fresh medium for four-to-six hours (WT remove cipro) compared with WT cells grown in cipro for 24 hours (WT cipro 24h). Scale bar, 10μM. Means ± range 2 experiments.

(E) Cipro induction of ROS requires SulA. Cells grown in MAC cipro (Table S1) were analyzed for ROS in log-phase cells with DHR ROS dye and flow cytometry. ROS-high cells, those within the gate illustrated (black horizonal bar). Means ± range, 2 experiments. *Different from no cipro, p<0.01, two-tailed Student's t-test.

(F) σ^S-high cells are reduced in SulA-defective cells. Cells grown in MAC cipro (Table S1) were analyzed by flow cytometry for σ^S activity from *yiaG-yfp*. σ^S-high cells, those within the gate shown (black bar, **Methods**). Means ± range, 2 experiments. *Different from WT, p<0.01, one-way ANOVA with Tukey's post-hoc test. Because both σ^S-high status is required for mutagenesis (Figure 3), and SulA is required for about half of mutant formation (Figure 7F and G), one might expect that the SulA-dependent half of the σ^S-high cells might generate mutants preferentially. Paradoxically, the σ^S-high cells remaining in the Δ*sulA* mutant appear to be neither enriched nor depleted for mutant-generating gamblers in that the number of σ^S-high cells (within our gate) is reduced by about the same amount as mutagenesis per-chromosome as follows. Δ*sulA* cells

showed a 2.4±0.6 times reduction in σ^S-high cells (8%±1% of Δ*sulA* cells compared with 19%±3% of WT cells) and a 1.8±0.4 times reduction in cipro-induction of per-chromosome mutation rate (4±0.5 times higher mutation rate with cipro/no cipro in Δ*sulA* cells compared with 7±1.5 times higher mutation rate with cipro/no cipro in WT cells). These reductions caused by Δ*sulA*—2.4±0.6 and 1.8±0.4—are not significantly different (p = 0.9, two-tailed Student's t-test), suggesting that the SulA-dependent and -independent fractions of σ^S-high cells may be equally mutable, and only their number is reduced by Δ*sulA*. Alternatively, the gate within which we quantify σ^S-high cells might be too low resolution. Only part of the gated σ^S-high cells might produce most mutants, and that part might be reduced by more or less than half. Thus, our estimation of reduction of the σ^S-high population is likely to contain noise that may skew the comparison with loss of mutation induction. The data support the conclusion (Figure 6H-J) that SOS response promotion of ROS-high cells is not via promoting HR (e.g., Figures 6J and 7I). Cells grown in MAC cipro were analyzed in log phase (16h). Means ± range, 2 experiments. *Different from no cipro, p<0.01, two-tailed Student's t-test.

(G) DSB-repair protein RuvC is not required for induction of ROS by cipro. The data support the conclusion (Figure 6H-J) that SOS response promotion of ROS-high cells is not via promoting HR (e.g., Figures 6J and 7I). Cells grown in MAC cipro were analyzed in log phase (16h). Means ± range, 2 experiments. *Different from no cipro, p<0.01, two-tailed Student's t-test.

(H) σ^S overproduction does not substitute for SulA. Cells grown in MAC cipro *p <0.01, one-way ANOVA with Tukey's post-hoc test; n.s., not significant.